Pergamon

Int. J. Heat Mass Transfer. Vol. 41, No. 10, pp. 1293–1301, 1998

Printed in Great Britain
0017–9310/98 $19.00+0.00

PII: 50017–9310(97)00153–1

Marangoni convection in binary drops in air cooled from below

F. L. A. GANZEVLES and C. W. M. VAN DER GELD†

Eindhoven University of Technology, Faculty of Mechanical Engineering, W-hoog 3.144, P.O. Box 513, 5600 MB Eindhoven, The Netherlands

(*Received* 17 *January* 1997 *and in final form* 15 *May* 1997)

Abstract—Marangoni convection in binary drops resting on a plate in quiescent air is studied. Water is used with low molar fractions of 2-butanol or ethanol. The droplets are homogeneously cooled from below with an initial temperature difference of 3.5 K. In the presence of air, the thermocapillary and concentration-gradients induced motions are mutually reinforcing. The latter motions last much longer than the time it takes for interfacial temperature gradients to become negligible. The Marangoni convection time increases with increasing concentration of alcohol if the volume concentration is less than 10 vol.%, levels off at higher concentrations and is higher for 2-butanol than for ethanol. The consequences for dropwise condensation in practical compact heat exchangers are investigated by measuring differences in temperature gradient histories during actual condensation processes. © 1998 Elsevier Science Ltd.

1. INTRODUCTION

If condensation occurs in the cooling process of exhaust gases, heat transfer rates are high as compared to those occurring without condensation. The main reason of this difference is the release of the enthalpy of condensation. The frequent 'drying' of parts of the condenser plate by large drops that slide off this plate is one of the reasons why dropwise condensation has higher transfer rates then filmwise condensation [1–6]. Another reason might be a reduced heat transfer resistance per drop by internal convection. If this convection is caused by surface tension gradients it is called Marangoni convection. This motion is possible in pure water drops as the partial water vapor pressure may vary along the interface because of the presence of inert gases. Van der Geld and Brouwers [7] investigated the effect of thermocapillary motion in water droplets for the condensation of air–steam mixtures on PVDF plates by an indirect method. Ganzevles and van der Geld [8] directly measured the occurrence of temperature gradients on the droplet for this case, see the typical example of Fig. 1. This measurement is made with an infrared camera, see Sections 2.1 and 3.3, of one side of a condenser plate. The window diameter is 66 mm. The air–steam mixtures flows from right to left in a channel with a cross-section of 2×400 mm^2. The coolant flows vertically upwards in rounded rectangular channels, dimensions 1.37×1.47 mm^2 with the shortest size in face of the gas mixture. More details will be given in Section 2.1. One coolant channel on the LHS in Fig. 1 is blocked as demonstrated by the higher temperatures. In Fig. 1 a relative cold path is easily recognized, caused by the roll-off of a large drop just prior to observation. The edges of droplets, indicated in Fig. 1, are determined from simultaneous video recordings and from the analyzing of consecutive frames in pixel-format. The motion of drops, due to coalescence or drainage, indicates drop contours much more clearly than stills. This is more fully discussed in Section 3.3. Each droplet has the highest temperature at the top, where it has close contact with the relatively warm gases, and has lower temperatures near the plate. So temperature gradients occur at the drop interface. It is concluded that thermocapillary convection is likely to occur in the dropwise condensation of a single component from air–vapor mixtures.

The question now addressed is what is to be expected if two components are condensed simultaneously, from a mixture containing non-condensables as well. In this case, the surface tension depends on temperature, T, and the concentration of the second condensable in the liquid, x, whence

$$\frac{\mathrm{d}\sigma}{\mathrm{d}s} = \frac{\partial\sigma}{\partial T}\cdot\frac{\mathrm{d}T}{\mathrm{d}s} + \frac{\partial\sigma}{\partial x}\cdot\frac{\mathrm{d}x}{\mathrm{d}s} \tag{1}$$

where s, the length along the drop surface, is taken to be positive if from bottom to top. Usually, $\partial\sigma/\partial T < 0$ and $\partial\sigma/\partial x < 0$, see Fig. 3. If cooling is from below, $\mathrm{d}T/\mathrm{d}s > 0$, and the first term on the RHS of equation (1) is negative and yields downflow as depicted in Fig. 2(a). This flow is purely thermocapillary flow. If the *saturation concentration* at each interface temperature is assumed, see Fig. 3‡, the concentration would be

† Author to whom correspondence should be addressed.

‡ The surface tension decreases nonlinearly with increasing alcohol concentration (see refs. [9, 10] and Appendix A) and decreases approximately linearly with increasing temperature [11, 12].

NOMENCLATURE

c_p	heat capacity at constant pressure [J kg^{-1} K^{-1}]
M	molar mass [kg kmol^{-1}]
r	radius [m]
s	length along the drop surface [m]
t	time [s]
T	temperature [K]
V_i	molar volume of component i [m^3 mol^{-1}]
V_i^σ	molar volume of component i at liquid–gas interface [m^3 mol^{-1}]
x_i	molar fraction of component i in the liquid phase.

Greek symbols

λ	thermal conductivity [W m^{-1} K^{-1}]
ρ	mass density [kg m^{-3}]
σ	surface tension coefficient [N m^{-1}]
τ	diffusion time [s]
ψ	volume fraction of component i.

Superscript

–	average.

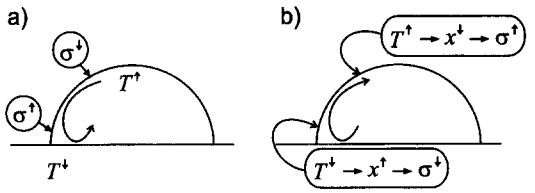

Fig. 2. Expected flow patterns in thermocapillary and destillocapillary case if the partial vapor pressure are homogeneous in the surrounding air.

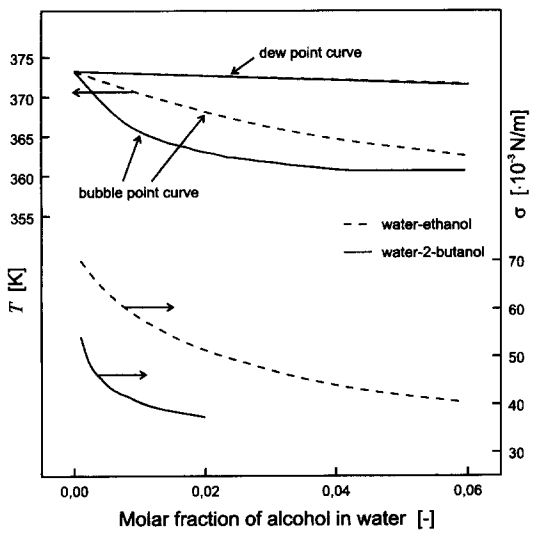

Fig. 3. Dew and bubble point curve at 0.103 MPa of alcohol in water. Surface tension at 298 K of two alcohol–water solutions. Based on data of refs. [9–12].

highest near the droplet foot, i.e. $dx/ds < 0$ and the second term on the RHS of equation (1) would be positive. This term would yield motion, named destillocapillary motion, from top to bottom, see Fig. 2(b). The combination of thermocapillary and destillocapillary motion may make $d\sigma/ds$ zero or even changing sign. This net effect of Marangoni motion is experimentally addressed in the present paper. Although thermocapillary convection in drops was studied by Zhang and Yang [13], Raake *et al.* [14], and Su and Yang [15], this was done for pure components only. Destillocapillary convection in drops was studied merely for isothermal conditions [16–19]. In the present study thermocapillary convection in binary drops is examined.

Individual drops are studied. The initial drop temperature is uniform in order to have a well-defined condition that might serve as reference case for other studies. The initial flat plate temperature is also uniform, but lower than the drop. The drop diameter is *ca.* 12 mm. The plate is continuously cooled from below. The thermocapillary motion [Fig. 2(a)] will be shown to be important only in the early stage of contact between drop and plate. The destillocapillary motion [Fig. 2(b)] will be shown to be dominant. These two actions will be seen to enhance each other rather than being counteracting. The temperature gradients, their evolution and the duration of initial motion will be quantified for various compositions of the binary mixtures and various concentrations of the more volatile component. The Marangoni flow patterns are categorized and velocities quantified to the extent that is necessary to understand and interpret the physical process. The results can easily be extrapolated to larger drop sizes.

To investigate the importance of these findings for practical applications, the temperature gradients occurring in the condensation of air–steam–ethanol mixtures in a PVDF compact heat exchanger are directly measured and discussed in the context of the other findings.

2. EXPERIMENTAL

2.1. *Test setup*

In Fig. 4 the test rig is given schematically. The droplet (6) lies horizontally on a black PMMA (poly-

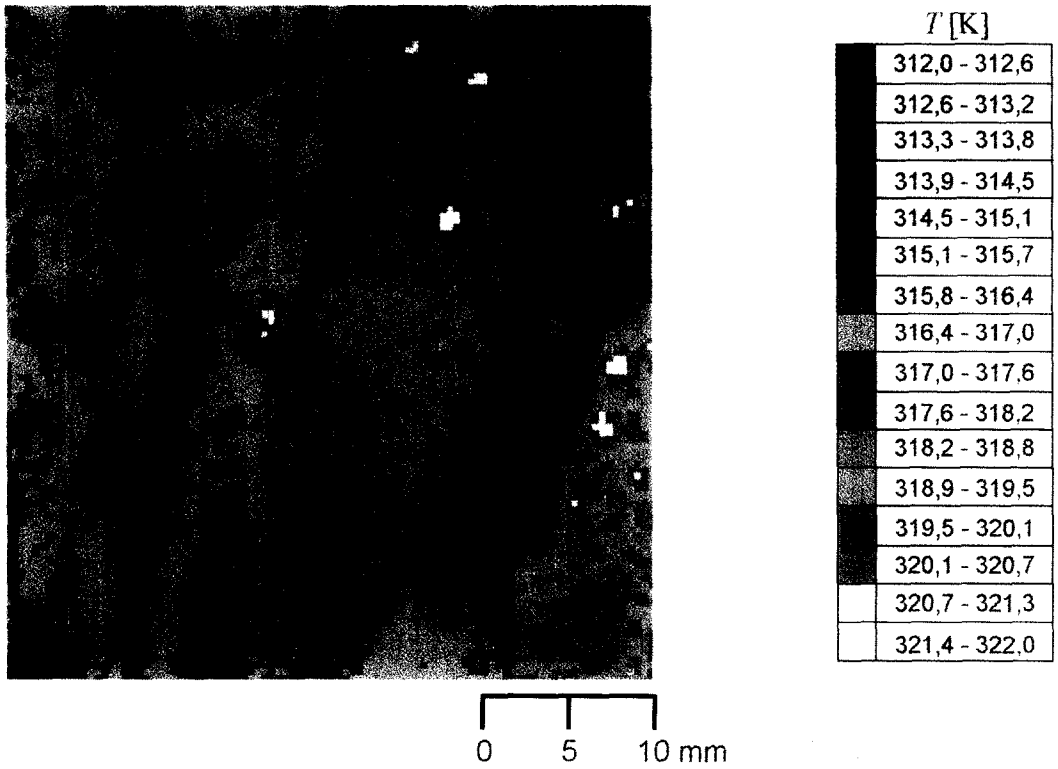

Fig. 1. Infrared image of temperatures of the interface of condensation drops and of condenser plate in-between. $T_{inlet} = 354.1$ K, $v_{inlet} = 5.6\ m\ s^{-1}$, air with 10 weight % vapor. Coolant: $T_{inlet} = 298.1$ K and mass flow rate 0.0246 kg s^{-1} per plate. No ethanol present.

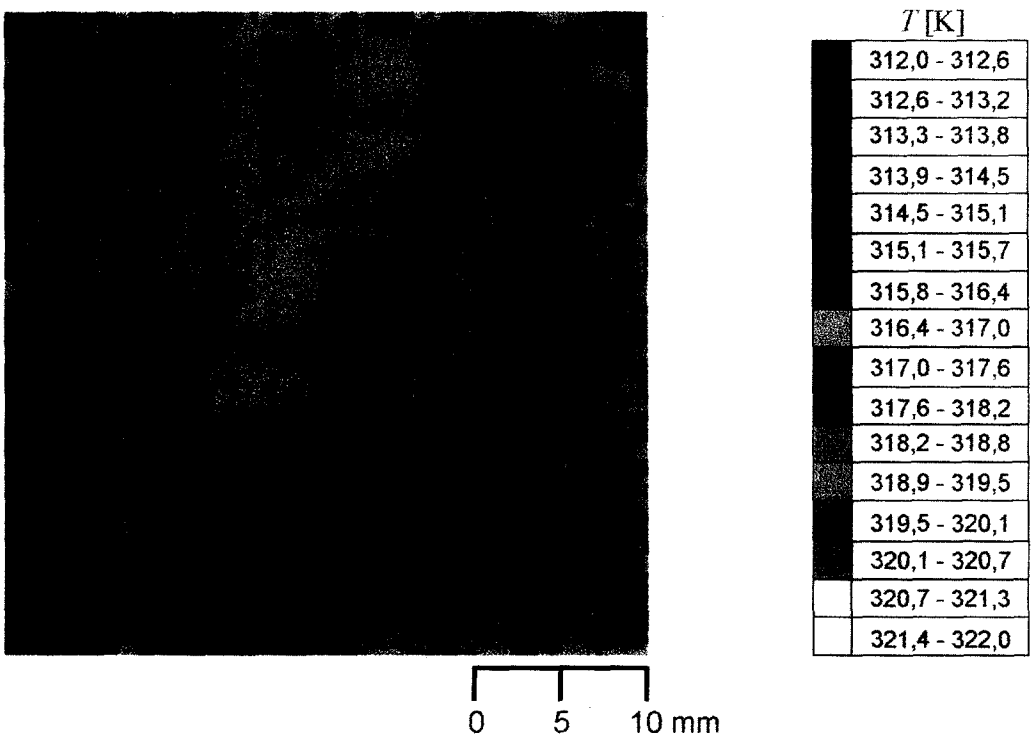

Fig. 9. Infrared image as that of Fig. 1, but with 0.14 weight % ethanol added to the air mixture. Other parameters: see Fig. 1.

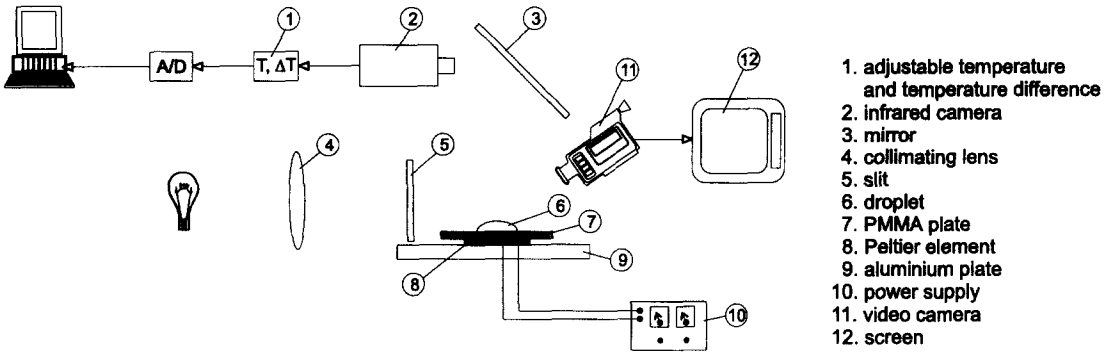

Fig. 4. Schematic of test module, lighting system and infrared camera.

methylmethacrylate) plate (7), 8.0 ± 0.1 mm in thickness. This plastic† has nearly the same thermal and surface properties as PVDF (polyvinylidene fluoride), which is used as condenser surface in the compact parallel plate heat exchanger used for Fig. 1 [7, 8]. The Peltier element (8), type CP 1.0-127-08L (Melcor Materials Electronic Products Corp., U.S.A.) $L \times W \times H$, $30 \times 30 \times 4$ mm^3, is glued between (7) and an aluminum plate (9), $L \times W \times H$, $240 \times 100 \times 10$ mm^3. The Peltier element cools the droplet from below and releases its heat to the aluminum plate. The current through and the voltage over the element are kept constant with a relative accuracy of 0.2%.

The temperature of the droplet gas–liquid interface‡ is measured contactless with an infrared camera (2), model thermovision system 680 (AGA infrared systems) spectral range 2.0–5.6 μm, with an 8° lens and two extension rings for maximum enlargement of the observed object. The golden mirror (3) reflects the infrared light from the droplet to the camera which is necessary because of the camera configuration. The detectable temperature is adjustable and the temperature range is selectable. The accuracy of the camera is 0.15 K for temperatures of about 300 K. The signal from the cooled detector, InSb in liquid nitrogen, is digitized and stored on hard disk (1) at a rate of 1.14 frames s^{-1}. Each image, 120×128 points, has actual dimensions 75×75 mm, which is 260 pixels per cm^2. This gives each point a width of 0.6 mm.

The flows and the diameters are measured using a video camera (11). The light source with a dimmed 400 W halogen lamp yields so-called 'cool' light in the sense that it does not affect the temperature of the observed object. This was verified with the infrared camera during special tests with a higher resolution bandwidth (2 K). The temperature rise during 600 s of irradiation was less than 0.1 K. Video recordings are made from above, aside and at an angle of 45° with the horizontal simultaneously.

The mixtures are prepared from demineralized water and ethanol (96%. $M = 46.07$ g mol^{-1}) or 2-butanol (purity at least 99.5%, $M = 74.12$ g mol^{-1}). The flows in the droplet are visualized with liquid crystals§ as tracers. The concentration of liquid crystals is about $5 \cdot 10^{-3}$ vol.%, which is negligible as compared to the other species.

2.2. *Measurement procedure*

A droplet is created on the PMMA plate using a 1.0 ml pipette. The diameter is measured on the screen by comparing the image with a reference object. The height of the droplets is 2.5 mm for the solutions with 8 vol.% or more alcohol and 2.9 mm for the other solutions. The diameter of the contact is 12 mm. The plate is cleansed with ethanol. After visual drying of the plate 1 min is waited before a droplet is created on the plate. It takes about 2 s after creation for a droplet of about 30 μl to become quiescent.

Each run lasts 175 s of infrared recording and 5 min of video recording. A bandwidth of 10 K has been used and the reference temperature of the non-cooled plate has been set to 295.8 K, measured with a contact thermometer (accuracy 0.1 K). The minimum detectable temperature difference is $\Delta T = 0.04$ K. The measured temperatures are in the range [286.4; 296.4 K] typically.

3. RESULTS AND ANALYSIS

3.1. *Results*

In the 20 experiments performed, the cooling power of the Peltier element has been kept constant (9.0 ± 0.1 W), the ambient temperature has been kept constant (295.8 ± 0.4 K) and the drop diameters are the same (12.0 ± 0.5 mm). Drops of pure water, water–ethanol and water–2-butanol solutions have been put on a flat, horizontal plate. The molar fractions are 0.0031;

† The thermal conduction coefficient is $\lambda_{PMMA} = 0.19$ W (m K)$^{-1}$, the heat capacity is $c_{p,PMMA} = 1.45$ kJ (kg K)$^{-1}$ and the mass density $\rho_{PMMA} = 1.18 \cdot 10^3$ kg m^{-3}. The contact angle of water or low concentration of ethanol or 2-butanol in water and PMMA is about 90°.

‡ The penetration depth of infrared light, in this range, is less than 0.1 mm, so the surface of the droplet is measured.

§ Type BM100/R29C4W/S33#11108-2A (Hallcrest, U.S.A.), mass density $\rho_{LC} = 998$ kg m^{-3} and an average diameter of 100 μm.

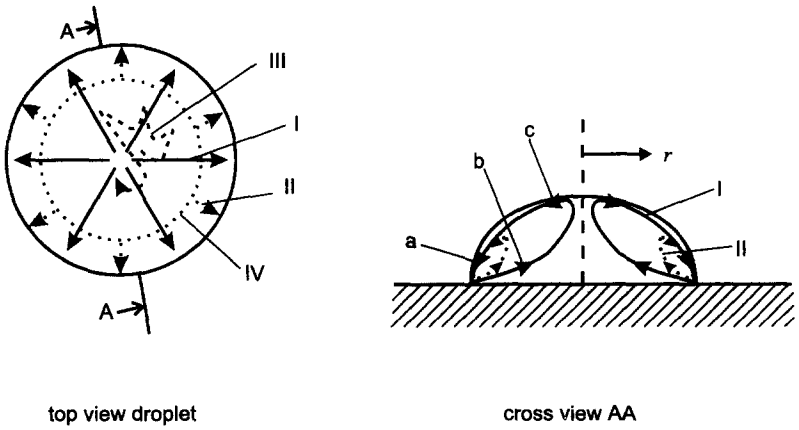

Fig. 5. Schematic of observed flow patterns inside a binary drop with a contact radius of 6 mm. I initial stage, II intermediate stage, defined in the text, III random walk-zone and IV boundary of II.

0.0063; 0.0127; 0.0262 and 0.0556 ($\pm$0.0003) for ethanol and 0.0020; 0.0040; 0.0082 and 0.0169 ($\pm$0.0002) for 2-butanol.

Tests without cooling by the Peltier element showed no motion in the drop for pure water, but gave convection patterns, named destillocapillary convection, in binary liquid drops. This motion mainly occurs in the vicinity of the contact line, the rim of the drop, i.e. in region II of Fig. 5. The destillocapillary convection lasts 130 s in a drop of 0.0020 2-butanol and 80 s in one of 0.0031 ethanol. These times of binary mixtures will be seen to be equal to those observed in drops put on a continuously cooled plate.

If the plate is cooled from below, before and after a drop is put on it, the flow pattern evolution depicted in Fig. 5 is observed. The flow patterns are irrespective of the drop composition although the magnitudes will be seen to differ. In the initial stage, large-scale motion occurs, indicated by I in Fig. 5. Later, in the intermediate state, this motion reduces to the near-rim motion II which has boundary IV. This boundary is roughly at a radial distance from the top, r, equal to 2/3 of the drop radius. This flow pattern is attained after *ca.* 1/3 of the total time of motion in the drop, named Marangoni velocity relaxation time. For pure water this relaxation time is 30 ± 1 s, in binary drops it is 75 s or more, as will be seen below. The relaxation time of pure water can be increased by 50% by increasing the initial water temperature by 7 K while retaining the same cooling power of 9 W [20]. In the intermediate stage, the motion near the top (III) is less organized and appears to be somewhat random. Probably small-scale instabilities occur in this area like the ones observed by, for example, Hoefsloot *et al.* [16].

With reference to Fig. 5, the magnitude of the velocities is highest near the contact line (a), 6–7 mm s^{-1} typically for the binary mixtures (highest for the 2-butanol solution) and up to 2 mm s^{-1} for pure water. The velocity of motion (c) is 1 to 2 mm s^{-1} typically, that in the bulk (b) is up to 0.5 mm s^{-1}. There is no need to further quantify the velocity field for the present study, as will become clear in Section 3.2.

Figure 6 shows typical temperature drop histories at various places at the interface of a drop of pure water, as measured with the infrared camera, see Section 2.1. ΔT is $T-T_{\text{plate}}$ with T_{plate} the temperature of the plate before the touch-down of the drop. After about 60 s the difference between the top and the rim of the droplet is about 1.3 K. The thermocapillary motion in this case is observed to stop after 30 ± 1 s, when *ca.* 50% of the temperature difference between top and foot has vanished. Similar temperature histories are measured for binary mixtures. In Fig. 7, typical temperatures at the top of the droplet are given for water–ethanol ($x = 0.0031$) and water–2-butanol ($x = 0.0020$) mixtures. The temperature drop at the top ($r = 0$) of the 2-butanol mixtures decreases most rapidly: after 80 s the temperature drop has become less then 0.5 K. For water or ethanol ($x = 0.0031$) the 0.5 K drop is only reached after 150 s.

The Marangoni relaxation times measured are collected in Fig. 8. The relaxation time increases with increasing molar fraction, but levels off and becomes

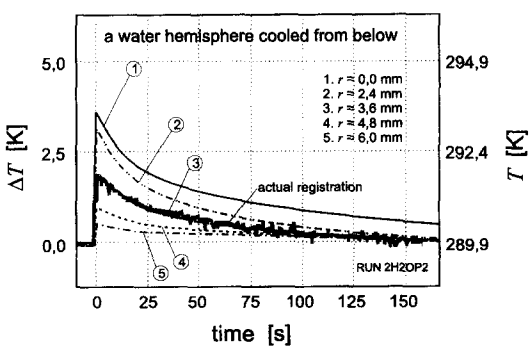

Fig. 6. Time histories of temperature at various locations at the interface of a pure water drop.

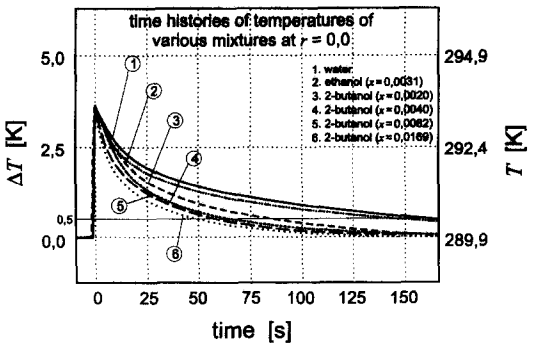

Fig. 7. Influences of species on the time histories of temperatures of the top of the droplet.

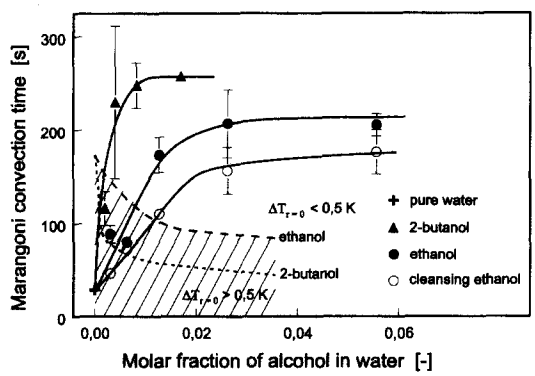

Fig. 8. Marangoni convection relaxation time vs concentration.

nearly independent of the concentration at quite a low molar fraction, 0.0020 for 2-butanol for example. The relaxation time of pure water, 30 s, is much less than the 125 s it takes for the temperature drop to become less than 0.5 K (see Fig. 6). In the shaded area of Fig. 8, below the line indicated by 'ethanol', the maximum temperature drop (at $r = 0$) is above 0.5 K for an ethanol–water drop of indicated concentration. In the non-shaded area the maximum temperature drop is less than 0.5 K for these binary drops. A similar border line is the dotted line in Fig. 8, indicated with '2-butanol'. These areas clearly show that the Marangoni relaxation time exceeds the time during which temperature drops are significant (larger than 0.5 K) by far, and that the difference between these two times is higher for 2-butanol than for ethanol. Two types of ethanol have been used. The one indicated 'ethanol' is pure (96 vol.%), the other 'cleansing ethanol' contains between 92 and 96 vol.% ethanol and up to 4 vol.% methanol.

To verify the importance of concentration gradients at the drop interface, a cotton wick, filled with 2-butanol, has been placed above a water drop without touching it. It induces weak motion near the edge (IV) even if the drop temperature is uniform. With some temperature drop the induced motion is higher. The direction of the flow is as indicated in Fig. 5.

3.2. *Analysis*

The tests show that Marangoni flows are established, mainly caused by concentration differences, see Fig. 8. This is named the destillocapillary effect. For all concentrations of volatile component the induced convection (see Fig. 5), has the same direction as the thermocapillary convection of pure water, see the left part of Fig. 2. For Marangoni convection, this can only be the case if the lowest concentration of the volatile component occurs at the foot of the drop, near the contact line where three phases meet. Consider a fluid element emanating at the interface at the top of the roll-cell (a) of Fig. 5. Before the fluid mixture particle arrives at the interface in the vicinity of the contact line it has been in contact with the ambient air for a relatively long time. By evaporation and subsequent diffusion in the air the fluid particle has become diluted with the more volatile component, which results in higher surface tensions near the contact line. On its way back to the top of roll-cell (a), the fluid particle is refreshed again by the bulk. Surface tensions are, therefore, lower at the top of (a). Motion is from regions with low surface tension to regions with high surface tension, as it should. The direction is always downward, as opposed to the expectations expressed in Fig. 2(b). This is possible because of evaporation in an ambient atmosphere that contains inert gases and, therefore, allows for a varying partial pressure of the volatile component at the interface.

The destillocapillary convection is self-sustaining since the velocities induced by the surface-tension gradients cause the mixture at the interface to be rich with 2-butanol in region III, near the top of the droplet, and poor near the contact line. The higher the initial concentration, the longer the continual refreshing of the mixture at places away from the drop foot can take place. This explains the increasing of velocity relaxation time with increasing concentration (see Fig. 8). At some molar fraction the Marangoni convection time becomes of the order of the typical diffusion time, and saturation sets in. This explains the leveling off of the curves in Fig. 8. A typical diffusion time, τ, may estimated by putting the Fourier number, $\lambda \cdot \tau / (\rho \cdot c_p \cdot r^2)$, equal by 1. This yields $\tau \approx r^2 \cdot \rho \cdot c_p / \lambda \approx 250$ s, which of the order of the times at which the curves in Fig. 8 start to level off.

Thermocapillarity is only active in the beginning of the time of motion in the droplet (see Figs. 7 and 8). It acts as an initiator of Marangoni convection whence the motion is more violent in the beginning of the time of motion. Once the motion is established the refreshing and evaporation continue the existence of surface-tension gradients.

The test with 2-butanol diffusing from a cotton wick positioned near the droplet shows that non-uniform diffusion of a volatile component to a stagnant liquid hemisphere provokes the same type of Marangoni

convection. This may well occur in many important applications, e.g. condensation in compact heat exchangers [7, 8]. Marangoni flow causes the drop to be cooled more rapidly then without this motion. In the absence of internal convection the droplet is cooled only by conduction, which is less effective. In the case of condensation droplet at a condenser plate, see Section 1, the temperature drop between the gas bulk and the top of the droplet would be increased by Marangoni convection which enhances the heat transfer. Whether this happens in actual condensation processes is investigated in the next section.

3.3. *Condensation of air–steam–ethanol mixtures in a PVDF compact heat exchanger*

Figure 9 shows a typical measurement result of condensation of an air–steam–ethanol mixture on a vertical PVDF condenser plate. This measurement is made with an infrared camera in the way described by Ganzevles and van der Geld [8]. Mixture flow is from right to the left, as revealed by some paths of large condensate droplets that ran down the plate and left a relatively cool path behind. The vertical, relatively warm, line on the LHS of the figure belongs to a blocked cooling channel (not cooled). The weight-percentage of ethanol per kg gas mixture is 0.14; the concentration steam is 0.10 kg kg mixture^{-1} at the inlet. Inlet gas velocity is 5.6 m s^{-1} in the 2 mm narrow slid between the condenser plate and the sapphire window. The diameter of the window is 66 mm. Some drop contours are indicated with black circles in Fig. 9. These contours are hard to be deduced from a single recording, like Fig. 9. A series of consecutive frames, each like Fig. 9, has been analyzed in order to discern drop motion which enables deduction of the droplet contour, see also Section 1. The rate of recordings is 1.14 frames s^{-1}, which is sufficient in view of the low departure rate of large drops [8]. A simultaneous video recording, of another condenser plate in the same condenser, provides additional information.

Comparison of this and similar recordings with recordings like Fig. 1, for an air–steam mixture, exhibits two main differences:

- the average drop size $\bar{r}$ is *ca.* 0.20 mm in the binary condensable case of Fig. 9, which is smaller than that of Fig. 1, where $\bar{r}$ is *ca.* 0.28 mm.
- The average temperature gradient along the interface of droplets, $\overline{\Delta T}/\bar{r}$, is somewhat less (4%) in Fig. 9 than in Fig. 1, indicating that mixing is better in binary drops than in (pure) water drops.

The first difference is due to the adhering force of drops on the plate being lower because of the lower surface tension of binary drops. The second difference is probably due to increased mixing by the destillocapillary effect, as explained in the previous sections. The reduction by internal convection of the drop heat resistance for condensation in practical circumstances (air–steam mixtures in a compact heat exchanger) has already been demonstrated by van der Geld and Brouwers [7] by an indirect method. The direct measurements presented here show that further homogenization of temperature is likely to occur in condensation drops of an air–steam–ethanol mixture condensing in a compact plate condenser. Figure 8 shows that only low concentrations are sufficient to achieve this.

In industrial condensation processes some heat transfer augmentation is to be expected if a low concentration volatile component is added to the gas mixture. Whether this effect would be economically interesting will be the subject of future research.

4. CONCLUSIONS

Marangoni convection in flat drops of a binary liquid in air has been studied. The liquid was water with low concentrations (up to 16 vol.%) of ethanol or 2-butanol. The plate on which the droplet rests is cooled from below. Inhomogeneous concentrations due to evaporation at the interface causes so-called destillocapillary convection even in the isothermal case. The liquid is inhomogeneously refreshed at the interface as a consequence of the roll-cells that develop there. The induced thermocapillary motion enhances the destillocapillary convection, lasts much shorter, but acts as a catalyst for the destillocapillary convection. In the presence of air, the two types of Marangoni convection are not conflicting (see Fig. 2).

For concentrations less than 10 vol.% the duration of the Marangoni convection depends on the initial concentration and is typically a few minutes if the droplet diameter is *ca.* 12 mm. Figure 8 summarizes these findings. Since the sustained Marangoni convection mainly occurs near the foot of the droplet (region II in Fig. 5), this duration is expected to be relatively independent of drop size as long as the drop diameter is not too small.

Temperature homogenization is measured of the condensate drops formed during condensation of steam–ethanol–air mixtures on a PVDF plate heat exchanger under practical process conditions. The homogenization is, on the average, found to be somewhat higher than that of condensation of steam–air mixtures (without ethanol). This is easily explained with the aid of the above findings.

Acknowledgement—The authors are grateful to SIOP (formerly SHELL International Petroleum Maatschappij B.V.) for financial support.

REFERENCES

1. Kast, W., Wärmeübertragung bei Tropfenkendensation. *Chemie Ingenieur Technik*, 1963, **35**, 163–168 (in German).
2. Tanner, D. W., Pope, D., Potter, C. J. and West, D., Heat transfer in dropwise condensation at low steam pressures in the absence and presence of non-condensable gas. *International Journal of Heat and Mass Transfer*, 1968, **11**, 181–190.

3. Rose, J. W. and Glicksmann, L. R., Dropwise condensation—the distribution of drop sizes. *International Journal of Heat and Mass Transfer*, 1973, **16,** 411–425.
4. Rose, J. W., Further aspects of dropwise condensation theory. *International Journal of Heat and Mass Transfer*, 1976, **19,** 1363–1370.
5. Tanaka, H., Further developments of dropwise condensation theory. *Journal of Heat Transfer*, 1979, **101,** 603–611.
6. Merte Jr, H. and Yamali, C., Profile and departure size of condensation drops on vertical surfaces. *Wärme- und Stoffübertragung*, 1983, **17,** 171–180.
7. van der Geld, C. W. M. and Brouwers, H. J. H., The mean heat resistance of dropwise condensation with flowing, inert gases. *Heat and Mass Transfer*, 1995, **30,** 435–445.
8. Ganzevles, F. L. A. and van der Geld, C. W. M., *In situ* measurements of wetting rate and local temperatures with dropwise condensation in a compact heat exchanger. *Proceedings of the 30th National Heat Conference*, HTD-314 Vol. 12. ASME, New York, 1995, pp. 68–76.
9. Reid, R. C., Prausnitz, J. M. and Poling, B., *Properties of Gases and Liquids*, 4th edn. McGraw-Hill, New York, 1987, pp. 648–651.
10. Tamura, M., Kurata, M. and Odani, H., Practical method for estimating surface tension of solutions. *Bulletin of the Chemical Society of Japan*, 1955, **28,** 83–88.
11. Jasper, J. J., The surface tension of pure liquid compounds. *Journal of Physics and Chemistry Reference Data*, 1972, **1,** 841–1009.
12. Landolt-Börnstein, *Zahlenwerte und Funktionen aus Physik, Chemie, Astronomie, Geophysik und Technik*, Teil 2a (6th edn). Springer, Berlin, 1960, p. 390 and p. 400.
13. Zhang, N. and Yang, W.-J., Evaporative convection in minute drops on a plate with temperature gradient. *International Journal of Heat and Mass Transfer*, 1983, **26,** 1479–1488.
14. Raake, D., Siekmann, J. and Chun, Ch.-H., Temperature and velocity fields due to surface tension driven flow. *Experiments in Fluids*, 1989, **7,** 164–172.
15. Su, Y.-J. and Yang, W.-J., Thermocapillary convection in evaporating sessile drops with internal solidifications. *Proceedings of the International Energy and Mass Transfer Conference*, paper 12-PC-02, ASME, New York, 1994, pp. 223–228.
16. Hoefsloot, H. C. J., Janssen, L. P. B. M. and Hoogstraten, H. W., Marangoni convection around a ventilated air bubble under microgravity conditions. *Chemical Engineering Science*, 1994, **49,** 29–39.
17. Velarde, M. G., *Physicochemical Hydrodynamics Interfacial Phenomena*, ed. M. G. Velarde, NATO ASI series, series B: Physics Vol. 174. Plenum Press, New York, 1988.
18. Marra, J. and Huethorst, J. A. M., Physical principles of Marangoni drying. *Langmuir*, 1991, **7,** 2748–2755.
19. Sørenson, T. S., Instabilities induced by mass transfer, low surface tension and gravity at isothermal and deformable fluid interface. In *Dynamics and Instability of Fluid Interfaces*, ed. T. S. Sørenson. Springer, Berlin, 1979, pp. 1–74.
20. den Boer, A. W. J. P., Marangoni convection: numerical model and experiments. Ph.D. thesis, Eindhoven University of Technology, Eindhoven, The Netherlands, 1996.
21. Westmeier, S., Exzeßenthalpie, Freie Exzeßenthalpie, Exzeßvolumen und Viskosität von ausgewählten binären flüssigen Mischungen, Teil IV: Die systeme Wasser–tertiäres Butanol und Wasser–sekundäres Butanol. *Chemische Technologie*, 1977, **29,** 218–222.

APPENDIX A

Surface tension of mixtures

The surface tension of aqueous binary mixtures is expressed by Reid [9] and Tamaru *et al.* [10] in terms of the surface tension, σ_i, of the components i ($i = 1, 2$):

$$\sigma_{\text{mix}} = (\psi_1^\sigma \cdot \sigma_1^{1/4} + \psi_2^\sigma \cdot \sigma_2^{1/4})^4. \tag{A1}$$

Here, $\psi_1^\sigma = x_i^\sigma \cdot V_i / V^\sigma$ denotes, what is named, the superficial volume fraction at the surface,

$$x_i = (\rho_i / M_i) \Big/ \sum_{j=1}^{n} (\rho_j / M_j)$$

the molar fraction of component i, V_i the molar volume of component i and

$$V^\sigma = \sum_{i=1}^{n} x_i \cdot V_i^\sigma$$

the total molar volume at the liquid–gas interface. V_i follows from the molar mass and the mass density, listed for 2-butanol by Westmeier [21].

The surface tensions of pure components are given by Jasper [11] and Landolt-Börnstein [12]. The following surface tension gradients are relevant for the present study:

$$\left.\frac{\partial \sigma}{\partial T}\right|_{H_2O} = -0.148 \cdot 10^{-3} \text{ N (m K)}^{-1},$$

$$\left.\frac{\partial \sigma}{\partial T}\right|_{C_2H_5OH} = -0.0832 \cdot 10^{-3} \text{ N (m K)}^{-1} \quad \text{and}$$

$$\left.\frac{\partial \sigma}{\partial T}\right|_{C_4H_9OH} = -0.0795 \cdot 10^{-3} \text{ N (m K)}^{-1}.$$